227-W output all-fiberized Tm-doped fiber laser at 1908 nm

Hu Zhen-Yue(胡震岳), Yan Ping(闫 平), Xiao Qi-Rong(肖起榕),
Liu Qiang(柳 强), and Gong Ma-Li(巩马理)†

Center for Photonics and Electronics, State Key Laboratory of Tribology, Department of Precision Instruments, Tsinghua University, Beijing 100084, *China*

(Received 12 February 2014; revised manuscript received 10 March 2014; published online 10 August 2014)

In this paper, we report that a diode-pumped thulium-doped double clad silica fiber laser can provide powers of up to 227 W at 1908 nm, corresponding to a slope efficiency of 54.3%, and an optical-to-optical efficiency of 51.2%. The output power, to the best of our knowledge, is the highest output at 1908 nm. The beam quality M^2 factor is about 1.56. Also discussed in this paper is the dependence of the laser performance on fiber length.

Keywords: thulium-doped fiber laser, rate equations, 1908 nm

PACS: 42.55.Ah, 42.55.Wd, 42.60.Mi **DOI:** 10.1088/1674-1056/23/10/104206

1. Introduction

Thulium-doped fiber lasers (TDFLs) producing high output power in the 2-μm spectral region have attracted much attention due to their numerous applications in the areas such as medical imaging, lidar, spectroscopy, etc.[1–5] And another important usage of TDFLs is the pumping source of Ho:YAG solid state laser.[6] Compared with the solid state laser pumping source, the TDFL has a better beam quality and is easy to operate.[7] As a pumping source of Ho:YAG, the TDFL needs to be tuned to produce a narrow 1908-nm emission peak. For cladding-pumped TDFL operating below about 1.95 μm, the signal reabsorption loss is a significant design concern which can create challenges for 1908-nm operation, and it is often observed as an instability.[8]

With the development of 790-nm laser diode (LD), it has become a main method to obtain 1908-nm output pumped by 790-nm diodes directly. And the TDFLs could reach 200% quantum efficiency theoretically due to the cross-relaxation process.[9] The master oscillator power amplifier (MOPA) method is an excellent method to obtain high power output, which also has been used to achieve high powers at 1908 nm. The highest 1908-nm thulium source pumped by 790 nm reportedly has been a 12.5-W oscillator and a 70-W MOPA.[10] However a MOPA is much more sensitive to external feedback from reflections such as Ho:YAG cavity optics. For this reason a laser rather than an MOPA is preferable for pumping Ho:YAG. For a higher power TDFL at 1908 nm, in 2008, Bennetts *et al*. obtained an output power of 110 W.[11] In order to achieve high power output, a dichroic mirror (HR at 790 nm) was placed at the end of the fiber to reflect the pumping light which could reduce the stability of the system.

In this letter, a high power TDFL pumped by 790-nm LDs is reported. We achieve a maximum output power of 227 W at 1908 nm for a launched pumped power of ∼ 443 W, a slope efficiency of 54.3%, and an M^2 factor of about 1.56. And it is the highest output at 1908 nm up to now.

The oscillator is more stable and less sensitive to external feedback from reflections for the fiber gratings than that of MOPA system. Also the oscillator is all fiberized, it is more compact and simple.

2. Experimental setup and results

The experimental setup for the TDFL is shown in Fig. 1. Seven fiber-coupled LDs were combined into one beamlet by using a 7×1 combiner. Each of the LDs generated a max output power of ∼ 70 W with a central wavelength of ∼ 790 nm and full width at half maximum (FWHM) of 1.66 nm as shown in Fig. 2. The LDs were cooled with thermoelectric module, so the LDs could work at right temperature.

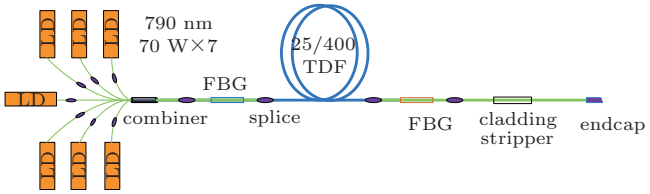


Fig. 1. (color online) System configuration of the 227-W all-fiberized TDFL.

The oscillator was based on a double-clad Tm-doped fiber with 25-μm, 0.09-NA circular core and 400-μm, 0.46-NA, octagonal inner-cladding, and its absorption coefficient at 790 nm was 4 dB/m. The active fiber was 3m long wrapped around a 28-cm diameter mandrel. The fiber was cooled at a constant temperature of 10 °C to provide thermal management and improve laser efficiency, because the performance of Tm^{3+} ions highly depended on temperature as a quasi-three-level system. A pair of fiber Bragg gratings (FBGs) at a wavelength of ∼ 1908 nm (one had high reflection $R = 99.7\%$,

†Corresponding author. E-mail: gongml@mail.tsinghua.edu.cn

© 2014 Chinese Physical Society and IOP Publishing Ltd

and the other had partial reflection $R = 10\%$) was separately spliced to each end of the Tm-doped fiber to complete a laser cavity. The Tm-doped fiber and all the other optical components were fusion spliced, providing an all-fiber configuration for the whole 1908-nm Tm-doped fiber laser system. The power loss of splice tested was about 0.1 dB, hence it improved the efficiency greatly.

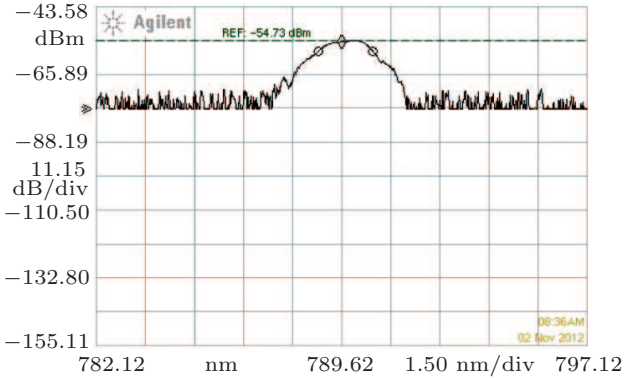


Fig. 2. (color online) Emission spectrum of LDs after the combiner: central wavelength of 789.62 nm and bandwidth (FWHM) of 1.66 nm.

Cladding stripper was used to remove residual pump light and signal light that leaked into the cladding, and we achieved up to 22 dB of attenuation for the light in cladding.

In our experiment, we found that the feedback would reduce the output greatly. In order to keep the stability of the oscillator, the feedback from the end facet must be reduced. In this experiment, the angle of the endcap was about 8° by cleaving.

The laser output power was measured with a power meter (OPHIR NOVA II : FL250A-LP1-SH-V1). The laser output power versus the pump power is plotted in Fig. 3. The threshold pump power was 12 W, and the maximal output power could reach 227 W at a launched power of 443 W. With increasing the pump power, the output power increased linearly. The slope efficiency was approximately 54.3%, an optical-to-optical efficiency was 51.2%, which exceeded the Stoke limit.

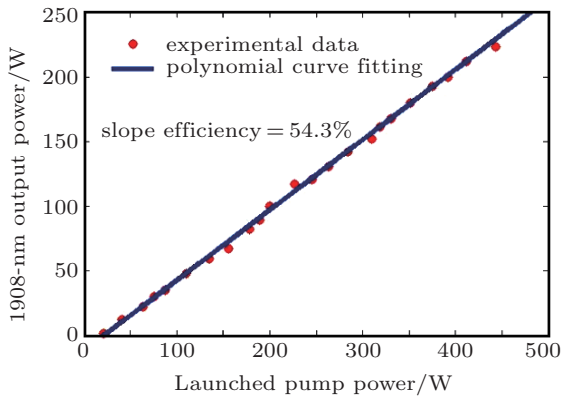


Fig. 3. (color online) Output power versus launched pump power.

The laser spectrum was measured with a spectral analyzer (Ocean Optics SpectraSuite NIRQuest-256: NQ21A0080) as shown in Fig. 4. The peak wavelength was 1907.8 nm. Because spectral resolution was 4 nm, we could not obtain an accurate bandwidth.

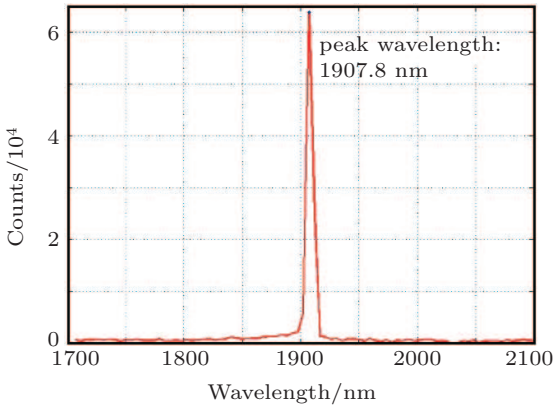


Fig. 4. (color online) Output spectrum of the TDFL.

The beam quality was measured in our experiment using the 90/10 knife-edge method. A lens ($f = 50$ mm) was located 53 mm away from the endcap. We measured the beam radius at 200 W. Figure 5 shows the measured beam radii at different positions after the lens. By fitting the Gaussian beam standard expression to these data, we estimated the beam quality to be $M^2 = 1.56$.

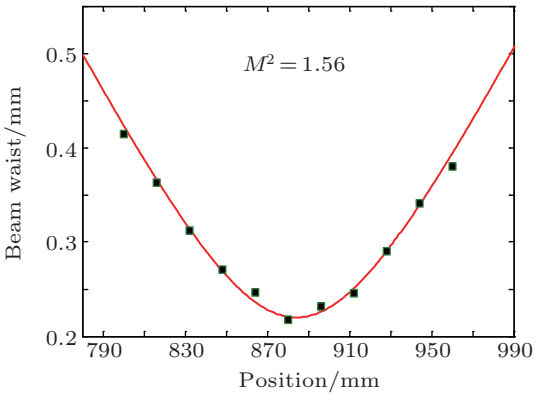


Fig. 5. (color online) Beam waist as a function of position after a focus lens with $f = 50$ mm at the output power of 200 W.

3. Discussion

In order to obtain high power output, we must choose a suitable fiber length, because shorter fibers will result in incomplete absorption, while longer fibers will lead to reduced efficiency, giving rise to the serious reabsorption losses at 1908 nm.

To examine the performance of the TDFL, with cross relaxation and ground state depletion taken into account, we construct a model for hard pumping at the $^3F_4$ energy (Fig. 6).

The rate equations for the local population densities of these levels at position z are as follows:[12,13]

$$\begin{cases} \dfrac{\mathrm{d}N_3}{\mathrm{d}t} = W_{03}N_0 - \dfrac{N_3}{\tau_3} - k_{3101}N_3N_0 + k_{1013}N_1^2, \\ \dfrac{\mathrm{d}N_1}{\mathrm{d}t} = 2k_{3101}N_3N_0 - 2k_{1013}N_1^2 - \dfrac{N_1}{\tau_1} \\ \qquad + \dfrac{\beta_{31}N_3}{\tau_3} - W_{10}N_1 + W_{01}N_0, \\ \dfrac{\mathrm{d}N_0}{\mathrm{d}t} = -W_{03}N_0 + k_{1013}N_1^2 - k_{3101}N_3N_0 \\ \qquad + \dfrac{N_1}{\tau_1} + \dfrac{\beta_{30}N_3}{\tau_3} + W_{10}N_1 - W_{01}N_0, \\ N \approx N_0 + N_1 + N_3, \end{cases} \tag{1}$$

$$\begin{cases} W_{03} = \dfrac{\lambda_\mathrm{p}\Gamma_\mathrm{p}}{hcA}\sigma_\mathrm{a}(\lambda_\mathrm{p})\left(P_\mathrm{p}^+(z) + P_\mathrm{p}^-(z)\right), \\ W_{10} = \dfrac{\lambda_\mathrm{s}\Gamma_\mathrm{s}}{hcA}\sigma_\mathrm{e}(\lambda_\mathrm{s})\left(P_\mathrm{s}^+(z) + P_\mathrm{s}^-(z)\right), \\ W_{01} = \dfrac{\lambda_\mathrm{s}\Gamma_\mathrm{s}}{hcA}\sigma_\mathrm{a}(\lambda_\mathrm{s})\left(P_\mathrm{s}^+(z) + P_\mathrm{s}^-(z)\right). \end{cases} \tag{2}$$

If we assume that the radial distributions of the pump and the signal power do not vary along the whole length of the fiber, the pump and the signal power can be described by

$$\begin{cases} \dfrac{\mathrm{d}P_\mathrm{p}^+(z)}{\mathrm{d}z} = -\Gamma_\mathrm{p}\left[N_0\sigma_\mathrm{a}(\lambda_\mathrm{p}) - N_1\sigma_\mathrm{e}(\lambda_\mathrm{p})\right]P_\mathrm{p}^+(z), \\ \dfrac{\mathrm{d}P_\mathrm{p}^-(z)}{\mathrm{d}z} = \Gamma_\mathrm{p}\left[N_0\sigma_\mathrm{a}(\lambda_\mathrm{p}) - N_1\sigma_\mathrm{e}(\lambda_\mathrm{p})\right]P_\mathrm{p}^-(z), \\ \dfrac{\mathrm{d}P_\mathrm{s}^+(z)}{\mathrm{d}z} = \Gamma_\mathrm{s}\left[N_1\sigma_\mathrm{e}(\lambda_\mathrm{s}) - N_0\sigma_\mathrm{a}(\lambda_\mathrm{s})\right]P_\mathrm{s}^+(z), \\ \dfrac{\mathrm{d}P_\mathrm{s}^-(z)}{\mathrm{d}z} = -\Gamma_\mathrm{s}\left[N_1\sigma_\mathrm{e}(\lambda_\mathrm{s}) - N_0\sigma_\mathrm{a}(\lambda_\mathrm{s})\right]P_\mathrm{s}^-(z), \end{cases} \tag{3}$$

where $\tau_1 = 334.7$ μs and $\tau_3 = 14.2$ μs are spontaneous lifetimes of the $^3\mathrm{F}_4$ and $^3\mathrm{H}_4$ respectively;[13] $\lambda_\mathrm{p} = 790$ nm and $\lambda_\mathrm{s} = 1908$ nm are pump and signal wavelengths; $k_{3101} = 3\times10^{-23}$ and $k_{1013} = 2.4\times10^{-24}$ are the cross-relaxation coefficients;[14] N_0, N_1, and N_3 are the population densities of the $^3\mathrm{H}_6$, $^3\mathrm{F}_4$, and $^3\mathrm{H}_4$ levels at the position z; $\sigma_\mathrm{e}(\lambda_\mathrm{p}) = 8\times10^{-25}$ m^{-2} and $\sigma_\mathrm{a}(\lambda_\mathrm{p}) = 8\times10^{-25}$ m^{-2} are the emission and absorption cross section of pump light; $\sigma_\mathrm{e}(\lambda_\mathrm{s}) = 5\times10^{-25}$ m^{-2} and $\sigma_\mathrm{a}(\lambda_\mathrm{s}) = 0.4\times10^{-25}$ m^{-2} are the emission and absorption cross sections of laser;[15] $P_\mathrm{p}^+(z)$ and $P_\mathrm{p}^-(z)$ are the pump powers in the forward and backward directions respectively; $P_\mathrm{s}^+(z)$ and $P_\mathrm{s}^-(z)$ are the signal powers in the forward and backward directions respectively; W_{03}, W_{10}, and W_{01} are transition rates; Γ_p and Γ_s are the pump and signal power filling distributions; A is the cross-section area of the core of fiber.

The boundary conditions are given by

$$\begin{cases} P_\mathrm{s}^+(0) = R_1P_\mathrm{s}^-(0), \\ P_\mathrm{s}^-(L) = R_2P_\mathrm{s}^+(L), \end{cases} \tag{4}$$

where L is the fiber length; $R_1 = 0.99$ and $R_2 = 0.1$ are the reflectivities at $z = 0$ and $z = L$ at 1908 nm respectively.

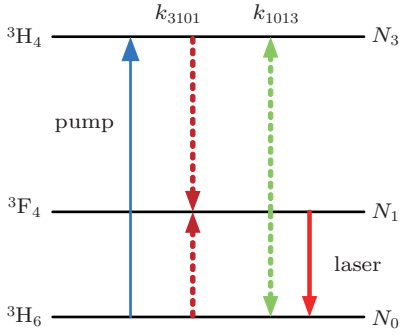


Fig. 6. (color online) Schematic view of $^3\mathrm{H}_6 \rightarrow {}^3\mathrm{H}_4$ pump scheme in Tm^{3+} ions.

The theoretical model is given by Eqs. (1)–(4). We calculate the frequency-dependent rate equation by the Runge–Kutta method. In a steady state,

$$\frac{\mathrm{d}N_3}{\mathrm{d}t} = \frac{\mathrm{d}N_1}{\mathrm{d}t} = \frac{\mathrm{d}N_0}{\mathrm{d}t} = 0,$$

and we obtain the position-dependent steady-state power and population density distribution.

The curves of output power versus fiber length at the different pump powers are shown in Fig. 7. It follows from this figure that the suitable fiber length is corresponding to the pump power and suitable fiber length increases with pump power increasing. If the fiber is too long, the output will decrease. When the pump power is around 500 W, the suitable fiber length is 3 m∼5 m.

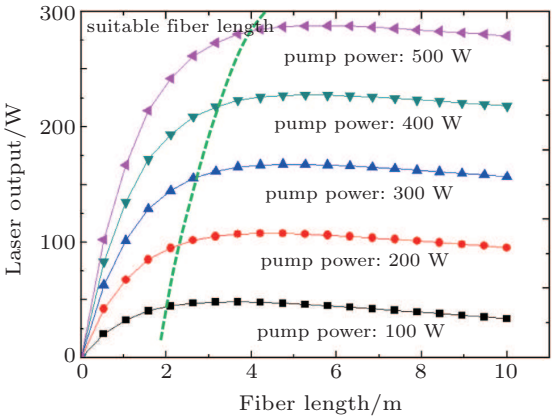


Fig. 7. (color online) Curves of output power versus fiber length at different pump powers, and the green dotted line is for the suitable fiber length at different pump powers.

In our experiment, the max incident pump power is 443 W, so we chose 3m long active fiber. Comparison between theoretical and experimental results is shown in Fig. 8. As can be seen from the figure, the numerical results basically accord with the experimental results. We believe that the main source of error is the choice of cross-relaxation coefficient, because we usually take the cross-relaxation coefficient to be a constant in calculation. In fact, cross-relaxation coefficient shows a linear dependence on dopant concentration.[16]

When we take the cross-relaxation coefficient associated with the dopant concentration as a scale factor, it can be more fitting to the experimental results, however, for determining the percentage factor more theoretical and experimental studies are needed.

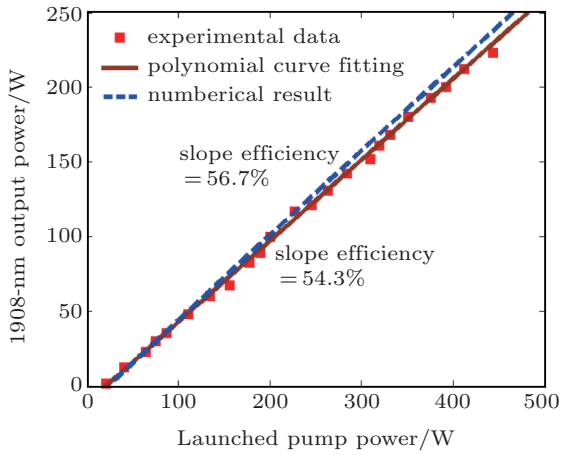


Fig. 8. (color online) Comparison between the numerical result and the experimental data.

4. Conclusions

In this paper we reported a high-power Tm-doped double clad silica fiber laser. Up to 227 W of output power at 1908 nm is obtained at a 443-W incident pump power, which is, to our knowledge, the highest output power, corresponding to a slope efficiency of about 54.3% and an optical-to-optical efficiency of 51.2%. In order to remove residual pump light and signal light that leaks into the cladding, a cladding stripper is used. And the beam quality $M^2 = 1.56$ is found. The oscillator is more stable and less sensitive to external feedback from reflections for the fiber gratings than that of MOPA system. Also the oscillator is all fiberized, and it is more compact and simple. In this paper, the dependence of the performance of the laser on the fiber length is discussed, and thus we could obtain a higher output.

References

[1] Kang H W, Lee H, Petersen J, Teichman J H and Welch A J 2006 *Proc. SPIE* **6078** 607815
[2] Budni P A, Pomeranz L A, Lemons M L, Miller C A, MostoJ R and Chicklis E P 2000 *J. Opt. Soc. Am. B* **17** 723
[3] Jansen E D, van Leeuwen T G, Motamedi M, Borst C and Welch A J 1994 *Lasers in Surgery and Medicine* **14** 258
[4] De Young R J and Barnes N P 2010 *Appl. Opt.* **49** 562
[5] Wang L, Fang T Z and Zhang L 2005 *Chin. Phys.* **14** 1423
[6] Kwiatkowski J, Jabczynski J K, Zendzian W, Swiderski J, Kaskow M and Gorajek L 2012 *Proc. SPIE* **8433** 84331J-1
[7] Clarkson W A, Shen D and Sahu J K 2006 *Proc. SPIE* **6100** 61000A-1
[8] Zhou R L, Ju Y L, Zhao J, Yang C and Wang Y Z 2013 *Chin. Phys. B* **22** 064208
[9] Jackson S D, Sabella A and Lancaster D G 2007 *Selec. Top. Quantum Electron.* **13** 567
[10] Frith G, Carter A, Samson B, Farroni J, Farley K and Tankala K 2008 in *Joint Conference of the Opto-Electronics and Communications Conference,* 2008 *and the* 2008 *Australian Conference on Optical Fibre Technology*, July 7–10, 2008, Sydney, Australia
[11] Bennetts S, Hemming A, Davidson A and Lancaster D G 2008 in *Joint Conference of the Opto-Electronics and Communications Conference,* 2008 *and the* 2008 *Australian Conference on Optical Fibre Technology*, July 7–10, 2008, Sydney, Australia
[12] Liao S Y, Gong M L and Zhang H T 2009 *Opt. Commun.* **282** 406
[13] Jackson S D and King T A 1999 *J. Lightwave Technol.* **17** 948
[14] Rustad G and Stenersen K 1996 *J. Quantum Electron.* **32** 1645
[15] Jackson S D 2010 *Proc. SPIE* **7686** 768608-7
[16] Taher M, Gebavi H, Taccheo S, Milanese D and Balda R 2012 *Proc. SPIE* **8257** 825707